Chemical stimulation of the *Arabidopsis thaliana* root using multi-laminar flow on a microfluidic chip

Matthias Meier,†* Elena M. Lucchetta‡ and Rustem F. Ismagilov*

Received 24th March 2010, Accepted 25th May 2010
DOI: 10.1039/c004629a

In this article, we developed a "plant on a chip" microfluidic platform that can control the local chemical environment around live roots of *Arabidopsis thaliana* with high spatial resolution using multi-laminar flow. We characterized the flow profile around the *Arabidopsis* root, and verified that the shear forces within the device (~10 dyne cm^{-2}) did not impede growth of the roots. Our platform was able to deliver stimuli to the root at a spatial resolution of 10–800 μm. Further, the platform was validated by exposing desired regions of the root with a synthetic auxin derivative, 2,4-dichlorophenoxyacetic acid (2,4-D), and its inhibitor *N*-1-naphthylphthalamic acid (NPA). The response to the stimuli was observed using a DR5::GFP *Arabidopsis* line, where GFP expression is coupled to the auxin response regulator DR5. GFP expression in the root matched the position of the flow-focused stream containing 2,4-D. When the regions around the 2,4-D stimulus were exposed to the auxin transport inhibitor NPA, the active and passive transport mechanisms of auxin could be differentiated, as NPA blocks active cell-to-cell transport of auxin. Finally, we demonstrated that local 2,4-D stimulation in a ~10 μm root segment enhanced morphological changes such as epidermal hair growth. These experiments were proof-of-concept and agreed with the results expected based on known root biology, demonstrating that this "root on a chip" platform can be used to test how root development is affected by any chemical component of interest, including nitrogen, phosphate, salts, and other plant hormones.

Introduction

Plants are sessile organisms that must adjust to numerous external environmental factors during their lifecycle.[1] A vital function of the root is uptake of water and chemicals from its environment.[2,3] In turn, roots exhibit a high plasticity in many developmental stages to comply with external environmental factors.[4] Although recent research has made progress in understanding the interplay between roots and their environment,[5–9] a central question remains: how does signaling occur between cells within the root upon receiving an environmental stimulus. By controlling the local chemical environment around the roots with high spatial and temporal resolution *in vitro*, we can obtain mechanistic insights into cell-to-cell signaling in response to a local environmental stimulus, such as nutrients or herbicides. The classical approach to control the chemical environment around roots or to chemically stimulate roots is to grow them on agar plates treated with the specific chemical environment or stimulus. However, this method is limiting in that it only allows spatial control on the order of a millimetre,[5,10] whereas developmental processes can depend on signaling between only a few cells on the scale of tens of microns. Furthermore, the spatial and temporal stabilities of chemical gradients are limited on agar plates. To solve these limitations, we developed and characterized a microfluidic platform based on laminar flow to create environments of different local chemical stimuli around a live *Arabidopsis thaliana* root.

Chemical stimulation of biological samples by multiple streams of laminar flow on the microscale has been established for a variety of cell types[11–13] and for whole model organisms.[14–16] However, maintaining culture conditions and stimulating biological samples on-chip for an extended period of time remain challenging.[17–19] Here, we designed a laminar flow-based microfluidic platform in polydimethylsiloxane (PDMS) to chemically stimulate particular cells within the roots of *Arabidopsis thaliana* while maintaining culture conditions over an extended period of time. The resolution of stimulation was ten microns, which is on the order of a single cell. A live root was introduced into the device through a microchannel perpendicular to the flow without dissection of the root from the plant. The leaves and stem of the plant were placed on an agar bed outside the device while the root was exposed to fluid flow, achieving long-term survival of the whole plant. Different chemical stimuli were delivered to different cells of the root by changing the flow solutions and the flow rate of three laminar streams relative to one another. The microfluidic platform was validated by stimulating a 10–20 μm segment close to the tip of an *Arabidopsis thaliana* root with the synthetic plant hormone 2,4-dichlorophenoxyacetic acid (2,4-D), a derivative of auxin, and the auxin transport inhibitor *N*-1-naphthylphthalamic acid (NPA).

Auxin is a hormone involved in many crucial processes in root development, such as maintenance of stem cell position at the

Department of Chemistry and Institute for Biophysical Dynamics, The University of Chicago, 929 E. 57th Street, Chicago, IL, USA. E-mail: r-ismagilov@uchicago.edu
† Current address: James Clark Center, 318 Campus Drive, Stanford University, Palo Alto, CA, USA. E-mail: matmeier@stanford.edu
‡ Current address: Columbia University Medical Center, Department of Genetics and Development, 701 W. 168th St HHSC 1130, New York, NY, USA.

root tip,[20] lateral root formation,[21] and root hair growth.[5] The hormone is further known to play a crucial role in transmitting environmental stimuli, such as gravity.[22] Several bacteria in the meta-environment of plant roots exhibit the ability to produce auxin, which they use to influence the development of the root.[23] Here, we externally applied 2,4-D and NPA by using laminar flow in a microfluidic chip to perturb the endogenous auxin profile of the root in a small segment. This microfluidic chip allows for high spatial and temporal resolution of environmental stimuli on the order of tens of microns. The response was observed in the neighboring, unstimulated root cells using a DR5::GFP *Arabidopsis* line,[24] in which GFP expression is coupled to the auxin response regulator DR5.

Experimental

Fabricating the microfluidic device

Two multilevel molds were fabricated by rapid prototyping in polydimethylsiloxane (PDMS) using SU-8 photoresist masters with different depths.[25] The channel geometry of the PDMS device is shown in Fig. 1. The three inlet channels in both the top and the bottom molds had widths of 400 μm, 50 μm, and 400 μm from left to right, respectively, and the main channel had a width of 800 μm. The top PDMS mold contained a channel with depth of 200 μm and alignment posts, and the bottom PDMS mold contained a channel with depth of 300 μm and alignment holes. The bottom mold also contained a root channel perpendicular to the main channel, at the point where the three inlets converged. This root channel was 100 μm in width and depth, and was used to hold the *Arabidopsis* plant, with the root protruding from the root channel into the flow. Both top and bottom PDMS molds contained two posts in the main channel with a width of 120 μm. These posts held the root that protruded from the root channel in place during flow.

Prior to assembly, the PDMS molds were placed in water for three days to remove non-polymerized PDMS from the molds.[26] Both PDMS molds were then baked over night at 120 °C, plasma oxidized, and attached to 0.2 mm thick, 1 × 3 inch glass slides.

Preparing the microfluidic device

An outlet was cut at the outer end of the root channel. The area on the glass slide surrounding the outlet was filled with 2% alginate solution. To form an agar bed around the outlet we used PDMS manufactured pieces to hold the alginate in position while it was being poured. Immediately after filling, several microlitres of plant media were added to the alginate solution in the root channel. The calcium concentration (8 mM) in the plant media was sufficient to cure the alginate solution. All channels of the bottom mold were then filled with sterile Murashige–Skoog media (Sigma Aldrich). Murashige–Skoog media were used for all experiments, and will herein be called plant media.

Growth of *Arabidopsis* plants

Arabidopsis DR5::GFP plants were germinated and grown for either 7 or 11 days on agar plates prepared with plant media before being transferred to the device. The typical size of an *Arabidopsis* root was 2 cm in length and 75 μm in diameter after 7 days of germination.

Placing *Arabidopsis* plants on the microfluidic device

The root was taken from the agar plate and positioned in the root channel in front of the stream posts in the main channel, with the leaves of the plant on the agar block at the outer end of the root channel. During transfer, care was taken not to squeeze or bend the root. To avoid leaking from the main channel into the root channel during flow, both ends of the root channel were sealed with alginate after the plant and root were in place. The top mold, with tubing inserted into the inlet channels, was inverted over the bottom mold and aligned by snapping the alignment posts into the alignment holes without damaging the root. The assembled molds were then clamped prior to the start of flow. To protect the plant from dehydration, the alginate block was kept hydrated with plant media during the experiment by adding drops of plant media onto the agar bed. Assembly of the device from the point of transferring the plant required one minute, and is summarized in Fig. 1.

Controlling and visualizing fluid flow

Three converging laminar streams were flowed through the device. Flow rates were controlled using syringe pumps (Harvard Apparatus). To visualize the laminar streams, we used plant media combined with either green food coloring (1 μL per 1 mL, McCormick) or 1 μm diameter fluorescent carboxy-FluoSpheres (0.5 mg mL^{-1}, Invitrogen). To prevent the fluorescent

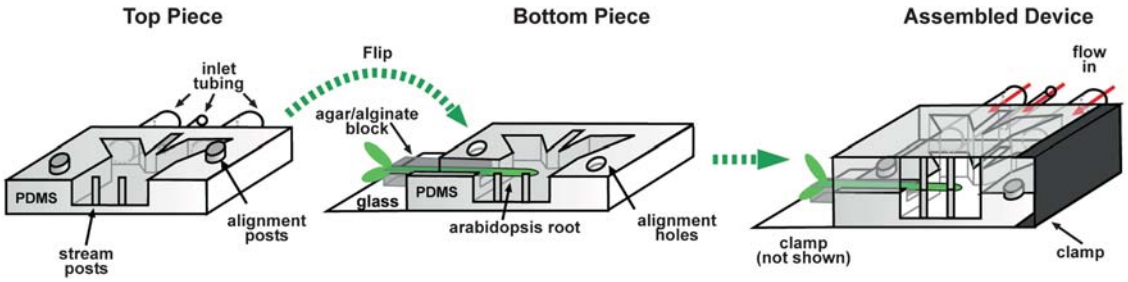

Fig. 1 Schematic of microfluidic device assembly around a live *Arabidopsis* root. A live *Arabidopsis* root was placed in a root channel filled with agar/alginate, located perpendicular to the main channel in a bottom PDMS mold. Both PDMS molds were attached to glass slides (glass slide for top mold is not shown). The top PDMS mold was then inverted over the bottom mold and the alignment posts were snapped into alignment holes to facilitate rapid assembly. The assembled device was then clamped and flow was started.

microspheres from attaching to the surface of the plant or the device, the carboxyl groups of the microspheres were deactivated with 1% bovine serum albumin (BSA) solution before use.

Stimulating root segments

Root segments were stimulated with either 2,4-D in plant media (25 μM, Sigma Aldrich) or *N*-1-naphthylphthalamic acid (NPA) in plant media (100 μM, Sigma Aldrich).

Image acquisition

Fluorescence and bright field images were obtained with a Leica DMI 6000 microscope coupled to a cooled CCD camera (ORCA ERG 1394, 12 bit, 1344 × 1024 resolution, Hamamatsu Photonics). MetaMorph Imaging System version 6.1r3 was used for image acquisition.

Data analysis

Data were analyzed using Matlab 7a. The GFP fluorescence intensity along the apical–basal axis of the root was quantified by cropping the root from the images and summing over the pixel intensity of each cross section. GFP fluorescence of the root at different time points was then normalized to the maximum GFP fluorescence intensity found at the root tip at time zero.

Results and discussion

Characterization of the flow profile around the *Arabidopsis* root

Reynolds numbers (*Re*) less than 2000, corresponding to laminar flow, can be easily achieved in simple channel geometries with a width of one millimetre.[27] To confirm laminar flow[27] in our device containing an *Arabidopsis* root, we visualized flow by adding fluorescence microspheres to the center stream. Fig. 2b shows the streamlines of the microspheres under different flow rates around a live *Arabidopsis* root in the main channel. A stable interface between the three streams was achieved over 8 hours at total flow velocities above 1 cm s^{-1} (~150 μL min^{-1}), where the $Re \approx 4$ in a rectangular duct. The flow around the root resembles the flow around a circular cylinder placed with its normal in the direction of flow. The stream pattern around a cylinder has been reviewed extensively and varies with the Reynolds number.[28] At moderate Reynolds numbers between 0.5 and 70, small eddies should form at the backside of the cylinder, possibly further enhanced by bends and rough surfaces of the root. Taking the direction of the flow to be the z direction, and length of the root to be in the x direction, we were mostly concerned about eddies or other flows that would induce mixing in the x direction, as such mixing would decrease the spatial resolution with which the root can be stimulated. By imaging in the x,z plane, we did not find evidence of such eddies or such mixing. We did not perform visualization of the flow patterns in the y direction to identify expected eddies that provide mixing primarily in the y,z direction, but those eddies should not significantly impact the resolution in these experiments.

To chemically stimulate segments of the root, auxin was added to the middle stream, and the width and position of the stream were adjusted by adjusting the flow rates of the outer streams

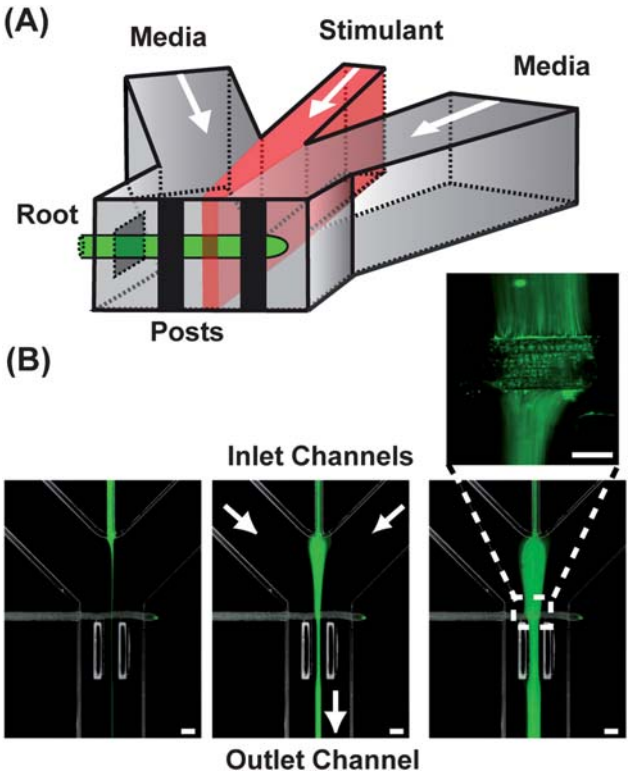

Fig. 2 Laminar flow around a live *Arabidopsis* root. (a) Schematic of the microfluidic platform for a chemical stimulation experiment. (b) Fluorescently labeled microspheres were used to visualize streamlines and width of the middle, flow-focused stream in the microfluidc channel around a DR5::GFP *Arabidopsis* root. The total flow rate in the experiments was 200 μL min^{-1}, where the ratios of the three inlets from left to right image were: 10 : 1 : 10, 5 : 1 : 5, and 2 : 1 : 2 (left : middle flow-focused : right stream). Scale bars are 200 μm. The width of the middle flow-focused streamed increased with decreasing flow rates of the outer stream from 5 to 90 μm. The zoomed image (scale bar 75 μm) shows the streamlines around the root segment. Bright field images were color inverted and overlaid with the corresponding fluorescence images.

(Fig. 2b). The width of the middle stream could be varied between 70 μm and 10 μm. A width of 70 μm was achieved using a flow rate of 50 μL min^{-1} for the two outer streams and 50 μL min^{-1} for the middle stream; a width of 10 μm was achieved using a flow rate of 200 μL min^{-1} for the two outer streams and 4 μL min^{-1} for the middle stream. A width of 10 μm is on the order of the average size of cells at the root tip. In all the following stimulation experiments, a total flow rate between 0.15 and 0.5 mL min^{-1} was used.

Verifying viability of the *Arabidopsis* root in the device over days

When introducing a live root to fluid flow, it is important to consider the shear stress of the streams and their possible influence on the viability of the organism. The shear stress acting on the root epidermis cells can be approximated by again making the assumption that the root is a cylinder. The steady-state fluid flow and shear stress around the cylinder were calculated using a commercial finite element package, FEMLAB 3.1 (Comsol Multiphysics), with the given channel geometry (300 × 800 μm) and a cylinder diameter of 75 μm. Under our experimental

conditions, on the surface of the cylinder the simulation revealed a maximum shear rate of ~1100 s^{-1}, corresponding to a shear stress of about ~10 dyne cm^{-2}. In comparison, in large arteries, the mean wall shear stress can typically be up to 40 dyne cm^{-2} in regions of uniform geometry.[29] Given the more robust cell wall of plants, we expected the root to be viable under these experimental shear stresses. To experimentally verify the viability of the *Arabidopsis* root in the device, the growth rate of the root was measured in the device. Ten plants were transferred to 10 devices and incubated with the device at 45° angle to the bench in a sterile Petri dish at room temperature over four days. In five of the ten devices, plant media were flowed with a total flow rate of 0.2 mL min^{-1} (which corresponds to a shear rate of 1100 s^{-1}) for 6 hours per day for four days. In the other five devices, flow was only applied for 1 minute per day to exchange the media. The average elongation rate of the roots in the device with and without extended periods of applied shear stress was 0.76 ± 0.3 mm per day and 0.80 ± 0.2 mm per day, respectively, which demonstrated that the root tissue was alive and the applied shear stresses had no influence on the viability of the root. However, when compared to roots growing on agar plates, the elongation rate of the roots decreased by 40% in the device. We have not investigated the cause of this discrepancy, but we assume that it was caused by the confinement of the root in the channel.

Chemical stimulation of the *Arabidopsis* root with the auxin derivative 2,4-D

To demonstrate environmental control around the *Arabidopsis* root using laminar flow, we first stimulated a root segment of DR5::GFP *Arabidopsis* with 2,4-D (Fig. 3a–d). In DR5::GFP plants, GFP expression is under control of the auxin-dependent promoter DR5, which is also susceptible to the auxin derivative 2,4-D. Endogenous auxin within the root tissue of DR5::GFP plants leads to a low expression level of GFP in pericycle cells, a cell group located around vascular cells of the stele in the center of the root, and high expression of GFP around the meristem cells, which are located at the root tip (Fig. 3a).[30]

In the 2,4-D stimulation experiment, all three laminar streams contained plant media, and the middle stream was focused on a 10–20 μm wide root segment 0.24 mm basipetal (towards the base of the stem) from the root tip. The positions of the three

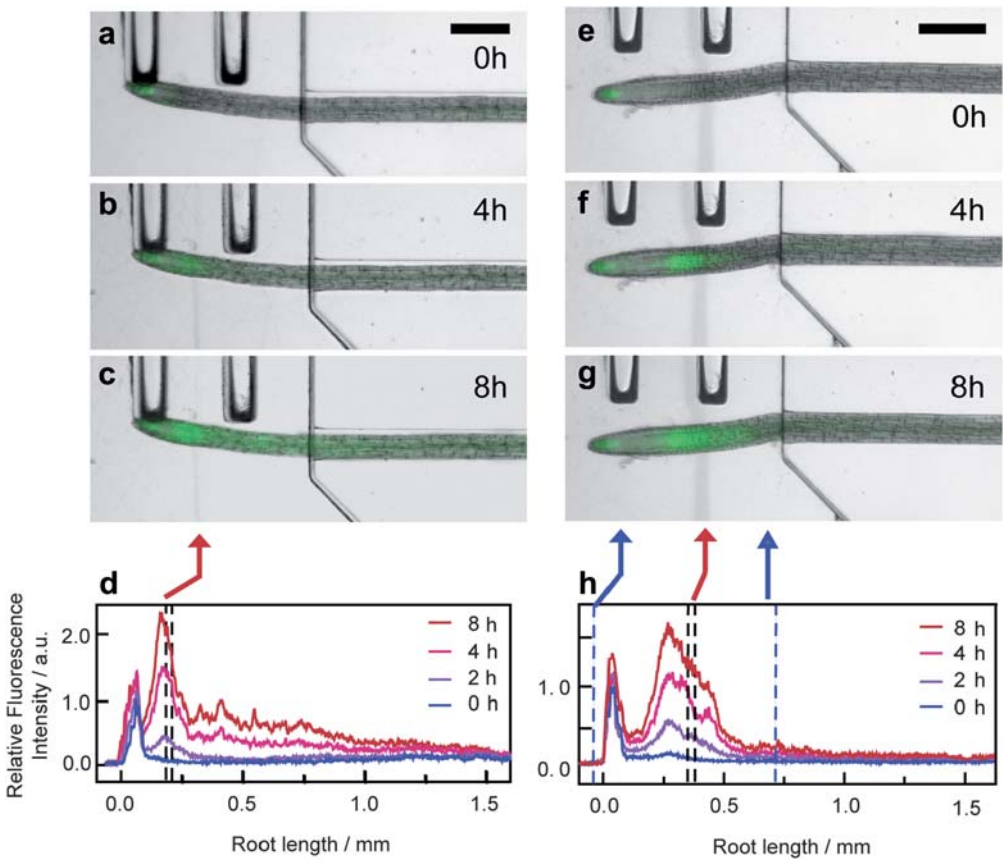

Fig. 3 Local 2,4-D stimulation of an *Arabidopsis* root segment using multi-laminar flow (a–c) and (e–g). Bright field images overlaid with the corresponding fluorescence images of a DR5::GFP *Arabidopsis* root after different time points of flow stimulation. Images are shown rotated 180° from the orientation in Fig. 2, to align the image with the *x*-axis in d and h. (a–c) The outer two streams contained plant medium, and the middle stream contained plant medium with 25 μM 2,4-D and food dye for visualization. (e–g) The outer two streams contained plant medium with 100 μM NPA, and the middle stream contained plant medium with 25 μM 2,4-D and a food dye for visualization. (d and h) GFP fluorescence changes in the root cells corresponding to the above 2,4-D or 2,4-D/NPA stimulation experiments plotted against the apical/basal axis of the root. Black and blue dotted lines in the plots denote areas of 2,4-D and NPA stimulation, respectively. Red arrows indicate location of 2,4-D stimulation and blue arrows indicate location of NPA stimulation. Scale bars = 250 μm.

streams were visualized by adding food dye to the center stream, and flow rates were adjusted to adjust the positions of the three streams. Food dyes had no effect on the viability of the root or fluorescence signal (data not shown). 2,4-D (25 μM) was added to the media solution of the middle stream. Fig. 3a–c shows the overlaid bright field and fluorescence images of the *Arabidopsis* DR5::GFP root in the microchannel at different time points of 2,4-D stimulation. To quantify the response to 2,4-D, total GFP fluorescence along the apical–basal axis of the root was plotted (Fig. 3d). After two hours of stimulation, an increase of GFP fluorescence in cells that were exposed to the middle stream containing 2,4-D was clearly observed. The GFP fluorescence increased in the cells exposed to 2,4-D, and also expanded in the basipetal direction over time during stimulation. After 8 hours of stimulation, the GFP fluorescence expanded from the cells directly exposed to 2,4-D to 1.6 mm in the basipetal direction. The GFP signal in the acropetal direction (towards the root tip) also increased over time, but with a much lower intensity as compared to the GFP signal in the opposite direction.

Induction of GFP expression in the root matched the position of the flow focused stream containing 2,4-D (a region of 20 μm) and thus this result demonstrated that 2,4-D was quickly and locally taken up by the root from the fluid. The early induced GFP signal within the root tissue stretched symmetrically over a segment of ~100 μm with the highest GFP signal at the position of the 2,4-D stream. Rapid diffusion of 2,4-D in the apoplast can explain the broadening of the GFP signal to an area of 100 μm after 2 hours of stimulation.[22] Interestingly, it has been approximated that after release in the apoplast, the auxin concentration decreases by a factor of 10 within about 42 μm.[31] The so-called decay length was calculated only on the basis of the membrane permeability and diffusion coefficient of 2,4-D. Considering diffusion in both directions from the stimulation area, we found that one decay length is sufficient to drop the 2,4-D concentration to a level where no GFP was expressed. After longer 2,4-D stimulation, the symmetric GFP expression profile was lost and GFP expression expanded strongly in the basipetal direction with time. This is in agreement with the well-described endogenous transport system of auxin in the close environment of the root tip.[32–35] Auxin membrane transporters actively shuttle auxins in the basipetal direction, which explains the lower acropetal increase of GFP measured here. Absolute concentrations of auxin cannot be given, but after 8 hours of stimulation, the GFP fluorescence around the meristem cells at the root tip increased to values twice as high as what is found under natural conditions.

An important advantage of the laminar flow technique is that stimulation is not limited to a single chemical component, but rather, different streams can be exploited for multi-component stimulation in adjacent segments of the root simultaneously. We repeated the above 2,4-D root stimulation experiment and added NPA (100 μM) to the two flanking streams (Fig. 3e–h). NPA inhibits the polar auxin transport system in the root.[36] The result of the experiment was plotted analogously to the previous experiment (Fig. 3h); here, a ~20 μm wide 2,4-D stream was used to stimulate an area 0.36 mm from the root tip. Fig. 3h indicates the same local GFP fluorescence increase after 2 hours of 2,4-D stimulation, as observed in the absence of NPA. However, after 8 hours, it was clearly seen that the GFP fluorescence increased only in a segment of 300 μm around the stimulation area, and the broad expansion in the basipetal direction was not detected, as evidenced by comparing the GFP profiles in Fig. 3d and h at approximately 0.5–0.75 mm. It is notable that NPA also diffuses in the apoplast, and after 8 h of stimulation, the segment adjacent to the area stimulated with 2,4-D presumably also contained a high NPA concentration. Nevertheless, the increased 2,4-D concentration in the stimulated segment led to a GFP fluorescence signal comparable to the signal found in the absence of NPA. Thus the local NPA concentration did not inhibit cellular uptake of 2,4-D. From this we can conclude that the basipetal expansion of auxin seen in the first experiment is indeed driven by active transport and is thus in agreement with the classical literature reports.[37,38]

Finally, we showed that the local 2,4-D increase could be exploited to enhance morphological changes in the development of the root with high spatial resolution. To do this, we applied 2,4-D to a small segment of the root, focusing on root hairs at the root tip (Fig. 4). Root hairs are formed by epidermal cells called trichoblasts. Growth rates of root hairs along the entire root can be promoted by auxin as shown on agar plates.[37] To show this phenomenon specifically in a small segment of the root, we grew wild-type *Arabidopsis* plants for 11 days on agar plates and transferred a plant with a clear hair bulge at 0.26 mm from the root tip to the device. The middle stream was adjusted to surround the hair bulge. After adjusting the flow conditions, 2,4-D (25 μM) was added to the middle laminar stream. Fig. 4a shows the laminar stream at the beginning of stimulation, with the middle stream visualized with a dye. Time-lapse images of the root segment with the trichoblasts cells upon 2,4-D stimulation are shown in Fig. 4b. After 15 minutes of 2,4-D stimulation, the hairs started to grow at a rate of approximately 2.5 μm min^{-1}. Control experiments with only plant media had no measurable effect during the time of observation. Root hair growth can be subdivided in two phases, with an initial phase of a low growth rate (0.2–0.5 μm min^{-1}) and a later phase of fast growth rate (1–2.5 μm min^{-1}).[39] In our case, we observed that after 2,4-D stimulation, the hair growth rate was in agreement with the later phase of root hair development. Further, we observed that hairs grew with the expected axial symmetry.[1] However, after 25 minutes, hair bulges with non-axial symmetry grew from the stimulated region. After 35 minutes, we stopped the flow of the streams and monitored the plant over 24 hours. The end point is shown in Fig. 4c. During the incubation time, it was clear that the root tip grew towards the upper channel wall of the PDMS chip. Nevertheless, the stimulated segment can easily be identified after this time due to cell expansion induced by the increased 2,4-D concentration (arrow in Fig. 4c). The stimulated segment contained root hairs with different lengths. Fig. 4c also demonstrates that only a small segment was stimulated rather than the whole root, as it would be on an agar plate. The experiment was reproducible using other root segments with hair bulges.

Conclusion

We used a microfluidic device to control the chemical environment of a live *Arabidopsis* root, the most common model organism in plant biology. The technique exploits multi-laminar flow, which can stimulate 10 to 800 μm long segments

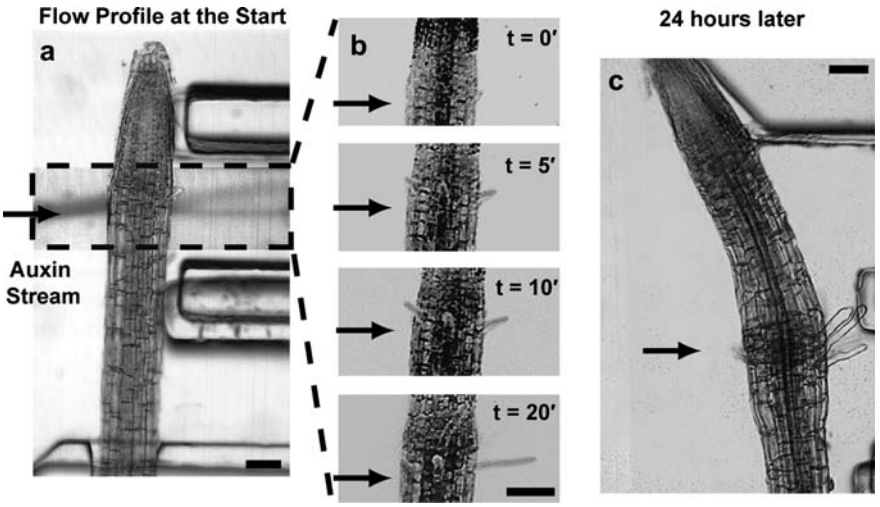

Fig. 4 Hair growth enhancement by local 2,4-D stimulation. (a) Flow condition around the live *Arabidopsis* root with position of the 2,4-D stream at the start of the experiment. (b) Zoomed in region of 2,4-D stimulation shows time lapse of hair growth after 0, 5, 10, and 20 minutes. (c) Images of the root taken 24 hours after the 2,4-D stimulation. Black arrows denote the position of the 2,4-D laminar stream. Scale bars = 50 μm.

of a live root in a microchannel. We demonstrated for the first time the biocompatibility and the survival of a live *Arabidopsis* root in a microfluidic device. The advantages of the laminar flow technique for local chemical stimulation and environmental control have been shown in a series of experiments, in which a 10–20 μm segment of the *Arabidopsis* root was stimulated by the auxin derivative 2,4-D. All experiments shown were designed as proof of principle, and our results on auxin transport and root hair growth induction matched expected results from literature. This validates the utility of such a system in elucidating other, unknown mechanisms. The presented technique is not limited to auxin, but rather, can be used for any chemical component of interest such as nitrogen, phosphate, salts, and other plant hormones to test local environmental factors during root development. Thus, the platform is of general interest for plant biology research. Microfluidic devices can be used to control microbes and microbial communities[40–42] and such approaches in combination with the device described here may elucidate the chemistry and biology of the plant–microbe interactions.[43,44] Additionally, chemical stimulation can easily be performed with temporal control by changing flow rates of the laminar streams. The platform developed herein can be expanded to control fluid flow around tens to hundreds of *Arabidopsis* roots at the same time to obtain higher statistical values for environmental factors during root development.

Acknowledgements

This work was supported in part by Grant 1R01GM0773301 from the NIH and by the NIH Director's Pioneer Award program (1DP1OD003584). M.M. was supported by the Alexander v. Humboldt Society. E.M.L. was supported by the Yen Postdoctoral Fellowship. We thank Prof. Jocelyn Malamy at the University of Chicago for DR5::GFP *Arabidopsis thaliana* seeds and scientific comments.

References

1 A. Bresinsky, C. Körner, J. W. Kadereit, G. Neuhaus and U. Sonnewald, *Strasburger-Lehrbuch der Botanik*, Spektrum Akad. Verl., 2008.
2 I. Casimiro, T. Beeckman, N. Graham, R. Bhalerao, H. Zhang, P. Casero, G. Sandberg and M. J. Bennett, *Trends Plant Sci.*, 2003, **8**, 165–171.
3 J. E. Malamy, *Plant, Cell Environ.*, 2005, **28**, 67–77.
4 A. Walter, W. K. Silk and U. Schurr, *Annu. Rev. Plant Biol.*, 2009, **60**, 279–304.
5 H. Zhang and B. G. Forde, *Science*, 1998, **279**, 407–409.
6 E. Baena-González, F. Rolland, J. M. Thevelein and J. Sheen, *Nature*, 2007, **448**, 938–942.
7 F. Rolland, E. Baena-Gonzalez and J. Sheen, *Annu. Rev. Plant Biol.*, 2006, **57**, 675–709.
8 A. Maruyama-Nakashita, Y. Nakamura, T. Tohge, K. Saito and H. Takahashi, *Plant Cell*, 2006, **18**, 3235–3251.
9 P. Achard, H. Cheng, L. De Grauwe, J. Decat, H. Schoutteten, T. Moritz, D. Van Der Straeten, J. Peng and N. P. Harberd, *Science*, 2006, **311**, 91–94.
10 S. Svistoonoff, A. Creff, M. Reymond, C. Sigoillot-Claude, L. Ricaud, A. Blanchet, L. Nussaume and T. Desnos, *Nat. Genet.*, 2007, **39**, 792–796.
11 A. M. Taylor, M. Blurton-Jones, S. W. Rhee, D. H. Cribbs, C. W. Cotman and N. L. Jeon, *Nat. Methods*, 2005, **2**, 599–605.
12 R. J. Taylor, D. Falconnet, A. Niemistö, S. A. Ramsey, S. Prinz, I. Shmulevich, T. Galitski and C. L. Hansen, *Proc. Natl. Acad. Sci. U. S. A.*, 2009, **106**, 3758–3763.
13 R. Gómez-Sjöberg, A. Leyrat, D. Pirone, C. Chen and S. Quake, *Anal. Chem.*, 2007, **79**, 8557–8561.
14 S. K. W. Dertinger, X. Jiang, Z. Li, V. N. Murthy and G. M. Whitesides, *Proc. Natl. Acad. Sci. U. S. A.*, 2002, **99**, 12542–12547.
15 S. Takayama, J. C. McDonald, E. Ostuni, M. N. Liang, P. J. Kenis, R. F. Ismagilov and G. M. Whitesides, *Proc. Natl. Acad. Sci. U. S. A.*, 1999, **96**, 5545–5548.
16 E. M. Lucchetta, J. H. Lee, L. A. Fu, N. H. Patel and R. F. Ismagilov, *Nature*, 2005, **434**, 1134–1138.
17 D. N. Breslauer, P. J. Lee and L. P. Lee, *Mol. BioSyst.*, 2006, **2**, 97–112.
18 J. El-Ali, P. K. Sorger and K. F. Jensen, *Nature*, 2006, **442**, 403–411.
19 G. M. Walker, H. C. Zeringue and D. J. Beebe, *Lab Chip*, 2004, **4**, 91–97.
20 T. Vernoux and P. N. Benfey, *Curr. Opin. Genet. Dev.*, 2005, **15**, 388–394.

21 B. Péret, B. De Rybel, I. Casimiro, E. Benková, R. Swarup, L. Laplaze, T. Beeckman and M. J. Bennett, *Trends Plant Sci.*, 2009, **14**, 399–408.
22 A. M. Rashotte, S. R. Brady, R. C. Reed, S. J. Ante and G. K. Muday, *Plant Physiol.*, 2000, **122**, 481–490.
23 S. Spaepen, J. Vanderleyden and R. Remans, *FEMS Microbiol. Rev.*, 2007, **31**, 425–448.
24 T. Ulmasov, J. Murfett, G. Hagen and T. J. Guilfoyle, *Plant Cell*, 1997, **9**, 1963–1971.
25 J. R. Anderson, D. T. Chiu, R. J. Jackman, O. Cherniavskaya, J. C. McDonald, H. Wu, S. H. Whitesides and G. M. Whitesides, *Anal. Chem.*, 2000, **72**, 3158–3164.
26 K. J. Regehr, M. Domenech, J. T. Koepsel, K. C. Carver, S. J. Ellison-Zelski, W. L. Murphy, L. A. Schuler, E. T. Alarid and D. J. Beebe, *Lab Chip*, 2009, **9**, 2132.
27 P. J. Kenis, R. F. Ismagilov, S. Takayama, G. M. Whitesides, S. Li and H. S. White, *Acc. Chem. Res.*, 2000, **33**, 841–847.
28 D. J. Tritton, *Physical Fluid Dynamics*, Oxford University Press, 1988.
29 P. F. Davies, *Physiol. Rev.*, 1995, **75**, 519–560.
30 J. Friml, E. Benková, I. Blilou, J. Wisniewska, T. Hamann, K. Ljung, S. Woody, G. Sandberg, B. Scheres, G. Jürgens and K. Palme, *Cell*, 2002, **108**, 661–673.
31 E. M. Kramer, *Plant Physiol.*, 2006, **141**, 1233–1236.
32 R. Swarup, J. Friml, A. Marchant, K. Ljung, G. Sandberg, K. Palme and M. Bennett, *Genes Dev.*, 2001, **15**, 2648–2653.
33 I. Blilou, J. Xu, M. Wildwater, V. Willemsen, I. Paponov, J. Friml, R. Heidstra, M. Aida, K. Palme and B. Scheres, *Nature*, 2005, **433**, 39–44.
34 E. M. Kramer and M. J. Bennett, *Trends Plant Sci.*, 2006, **11**, 382–386.
35 R. C. Bean, W. C. Shepherd and H. Chan, *J. Gen. Physiol.*, 1968, **52**, 495–508.
36 M. Jacobs and P. Rubery, *Science*, 1988, **241**, 346–349.
37 M. H. M. Goldsmith, *Annu. Rev. Plant Physiol.*, 1977, **28**, 439–478.
38 G. K. Muday and A. DeLong, *Trends Plant Sci.*, 2001, **6**, 535–542.
39 L. Dolan, C. Duckett, C. Grierson, P. Linstead, K. Schneider, E. Lawson, C. Dean, S. Poethig and K. Roberts, *Development*, 1994, **120**, 2465–2465.
40 H. J. Kim, J. Q. Boedicker, J. W. Choi and R. F. Ismagilov, *Proc. Natl. Acad. Sci. U. S. A.*, 2008, **105**, 18188–18193.
41 J. Q. Boedicker, M. E. Vincent and R. F. Ismagilov, *Angew. Chem., Int. Ed.*, 2009, **48**, 5908–5911.
42 F. K. Balagadde, L. You, C. L. Hansen, F. H. Arnold and S. R. Quake, *Science*, 2005, **309**, 137–140.
43 K. A. Cloud-Hansen, S. B. Peterson, E. V. Stabb, W. E. Goldman, M. J. McFall-Ngai and J. Handelsman, *Nat. Rev. Microbiol.*, 2006, **4**, 710–716.
44 P. Bonfante and I. A. Anca, *Annu. Rev. Microbiol.*, 2009, **63**, 363–383.